14. Farrell, M. J. *et al. HIRA*, a DiGeorge syndrome candidate gene, is required for cardiac outflow tract septation. *Circ. Res.* **84,** 127–135 (1999).
15. Kirby, M. L. in *Heart Development* (eds Harvey, R. P. & Rosenthal, N.) 179–193 (Academic, San Diego, 1999).
16. Kurihara, Y. H. *et al.* Aortic arch malformations and ventricular septal defects in mice deficient in Endothelin-1. *J. Clin. Invest.* **96,** 293–300 (1995).
17. Yanagisawa, H. *et al.* Role of Endothelin-1/Endothelin-A receptor-mediated signaling pathway in the aortic arch patterning in mice. *J. Clin. Invest.* **102,** 22–33 (1998).
18. Iida, K. *et al.* Essential roles of the winged helix transcription factor MFH-1 in aortic arch patterning and skeletogenesis. *Development* **124,** 4627–4638 (1997).
19. Liu, P., Zhang, H., McLellan, A. Vogel & Bradley, A. Embryonic lethality and tumorigenesis caused by segmental aneuploidy on mouse chromosome 11. *Genetics* **150,** 1155–1168 (1998).
20. Matzuk, M. M., Finegold, M. J., Su, J. G., Hseuh, A. J. & Bradley, A. α-inhibin is a tumour-suppressor gene with gonadal specificity in mice. *Nature* **360,** 313–319 (1992).
21. Baldini, A. & Lindsay, E. A. in In Situ *Hybridization Protocols* (ed. Choo, K. H. A.) 75–85 (Humana, Clifton, New Jersey, 1994).
22. Kaufman, M. H. *Atlas of Mouse Development* (Academic, San Diego, 1992).
23. McLeod, M. J. Differential staining of cartilage and bone in whole mouse fetuses by alcian blue and alizarin red S. *Teratology* **22,** 299–301 (1980).
24. Kidd, P. M. & Nicholson, J. K. in *Manual of Clinical Laboratory Immunology* 5th edn (eds Rose, N. R., deMacario, E. C., Folds, J. D., Lane, H. C. & Nakamura, R. M.) 229–244 (ASM, Washington DC, 1997).
25. Kruisbeek, A. M. & Shevach, E. in *Current Protocols in Immunology* Sections 3.12.1–3.12.14 (John Wiley and Sons, New York, 1991).
26. Kruisbeek, A. M. in *Current Protocols in Immunology* Sections 3.1.1–3.1.5 (John Wiley and Sons, New York, 1993).

Acknowledgements

We thank D. Su, Y. Wang and N. R. Parikh for technical assistance. This work was funded by grants from the NIH. A. Bradley is an investigator with the Howard Hughes Medical Institute.

Correspondence and requests for materials should be addressed to A. Baldini (e-mail: baldini@bcm.tmc.edu).

Polycystin-L is a calcium-regulated cation channel permeable to calcium ions

Xing-Zhen Chen*†, Peter M. Vassilev†‡, Nuria Basora*, Ji-Bin Peng*, Hideki Nomura*, Yoav Segal*, Edward M. Brown‡, Stephen T. Reeders*, Matthias A. Hediger* & Jing Zhou*

** Renal and ‡ Endocrine-Hypertension Divisions and Membrane Biology Program, Department of Medicine, Brigham and Women's Hospital and Harvard Medical School, Boston, Massachusetts 02115, USA*
† These authors contributed equally to this work

Polycystic kidney diseases are genetic disorders in which the renal parenchyma is progressively replaced by fluid-filled cysts[1]. Two members of the polycystin family (polycystin-1 and -2) are mutated in autosomal dominant polycystic kidney disease (ADPKD)[2–5], and polycystin-L is deleted in mice with renal and retinal defects[6]. Polycystins are membrane proteins that share significant sequence homology[6,7], especially polycystin-2 and -L (50% identity and 71% similarity). The functions of the polycystins remain unknown. Here we show that polycystin-L is a calcium-modulated nonselective cation channel that is permeable to sodium, potassium and calcium ions. Patch-clamp experiments revealed single-channel activity with a unitary conductance of 137 pS. Channel activity was substantially increased when either the extracellular or intracellular calcium-ion concentration was raised, indicating that polycystin-L may act as a transducer of calcium-mediated signalling *in vivo*. Its large single-channel conductance and regulation by calcium ions distinguish it from other structurally related cation channels.

Polycystin-L (PCL) and polycystin-2 share similarities in sequence, domain organization and/or membrane topology[6] (Fig. 1a) with cation channels such as the transient receptor potential (TRP) and voltage-gated Ca^{2+}, Na^+ and K^+ channel families[5,6,8–10]. Therefore, we utilized the *Xenopus* oocyte expression system to test whether PCL functions as a channel.

Oocytes injected with RNA encoding full-length PCL exhibited a 10-fold increase in total conductance, compared to water-injected oocytes, in NaCl-containing solution ($18.5 \pm 0.8\,\mu S$ versus $1.9 \pm 0.2\,\mu S$; Fig. 1b). Identical outward currents were obtained with 50 or 100 mM external Cl^- (Fig. 1c), suggesting that they are due to cation (predominantly K^+) efflux and not to Cl^- influx. Inward currents were largely abolished by replacing external Na^+ with *N*-methyl-D-glucamine (NMDG; Fig. 1d). PCL exhibited similar permeabilities (*P*) to Na^+, K^+ and Rb^+, lower permeability to Li^+ ($P_{Na} : P_K : P_{Rb} : P_{Li} = 1 : 0.98 : 0.97 : 0.87$), and very low permeabilities to large cations such as NMDG, tetraethylammonium or choline (Fig. 1d).

Single-channel analysis of 102/127 cell-attached patches of PCL-injected oocytes, but not 50/50 H_2O-injected oocytes or those

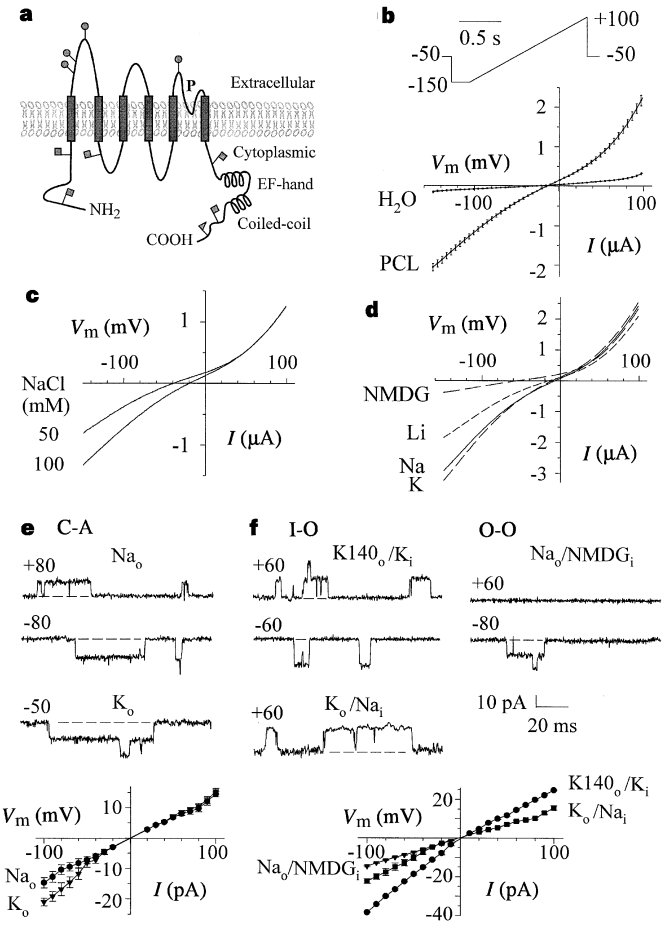

Figure 1 PCL channel conductance in the resting state. **a**, Proposed membrane topology for PCL. 'P' and circular, triangular and square flags indicate, respectively, the pore region, N-glycosylation, PKA- and PKC-phosphorylation sites. **b**, Average current–voltage (*I–V*) curves obtained from H_2O-injected ($n = 16$) or PCL-expressing ($n = 47$) oocytes, following a voltage ramp (top) in NaCl-containing solution. **c**, Comparison of currents obtained from the same oocyte in NaCl-containing solution and when 100 mM mannitol replaced 50 mM NaCl. **d**, Ion-selectivity *I–V* curves obtained using cation-Cl-substituted solutions. 2 mM KCl was removed from all solutions. **e**, Upper panels, selected recordings of PCL single-channel currents at indicated voltages (in mV) in the cell-attached (C-A) configuration. Dashed lines represent currents of the close state. Lower panel, average *I–V* relations ($n = 5$). The bath solution was 'Na_o'. **f**, Upper panels, PCL channel activities in inside-out (I-O) or outside-out (O-O) patches. Lower panel, average *I–V* relations ($n = 5$–10) obtained in I-O and O-O modes.

expressing other membrane proteins ($n = 40$), revealed a channel that is highly permeable to Na^+ and K^+ (Fig. 1e). The main unitary conductance at ± 50 mV in the presence of 100 mM external Na^+ was 137 ± 7 pS ($n = 8$). In the presence of external NaCl, excised patches only exhibited inward currents when intracellular cations were replaced by NMDG (Fig. 1f), indicating that PCL is impermeable to Cl^- and NMDG. Our data indicate that the outward currents observed in the cell-attached and whole-cell configurations were carried mainly by K^+, and that PCL functions as a nonselective cation channel.

We investigated divalent cation permeation, and found a multiphasic response when we raised extracellular Ca^{2+} (Ca_o^{2+}). In PCL-expressing oocytes pre-incubated in Ca^{2+}-free solutions for 3–5 min, large currents were evoked by adding 5 mM Ca_o^{2+} (Fig. 2a, b). At –50 mV, currents reached a peak 15–30 s after Ca_o^{2+} was added and then decreased to below basal levels with a time constant of 0.6 ± 0.1 min ($n = 17$; Fig. 2a). Ca^{2+} entry, determined by ^{45}Ca uptake, was markedly higher during the first 3-min period than during the second period (Fig. 2b). However, re-applying 5 mM Ca_o^{2+} inhibited inward currents. Thus, applying Ca_o^{2+} evoked activation and subsequent desensitization of PCL conductance, as assessed by whole-cell current and Ca^{2+} entry into oocytes. When Ca_o^{2+} was removed immediately after activation, the conductance during desensitization (dashed curve) was larger than before activation (point 1, fig. 2a). Desensitization was, however, reversible, as Ca^{2+}-induced activation recovered after 5–10 min incubation without Ca_o^{2+}.

To determine whether Ca^{2+} induces PCL-specific activation, we eliminated endogenous Ca^{2+}-activated Cl^- currents[11,12] by pre-incubating oocytes in Cl^--free solutions (Cl^- replaced by Hepes, gluconate or glutamate) for 10–24 h and using Na-glutamate- or mannitol-substituted solutions during measurements. Substantial increases in Ca^{2+}-activated current still occurred (Fig. 2c), indicating that the PCL-specific cation conductance was increased by Ca_o^{2+}. Hereafter, we define PCL channel activity as being in the resting, activated or desensitized state under the conditions corresponding to points 1, 2 and 3 in Fig. 2a, respectively.

As PCL is nonselectively cation permeable, we estimated the contributions of Ca^{2+} and Na^+ to the observed Ca^{2+}-activated inward current by simultaneously measuring whole-cell current and ^{45}Ca influx under voltage clamp (Fig. 2d, left panel). In oocytes deprived of Cl^- by incubation in Cl^--free solutions, Ca^{2+} entry accounted for most of the total Ca^{2+}-activated current in mannitol-substituted solution and only 20% in Na-glutamate-substituted solution (Fig. 2d, right panel), indicating that Na^+ and Ca^{2+} may compete for a common permeation pathway. In the latter case, the remaining 80% of Ca^{2+}-activated currents must result from Na^+ entry. Thus, with 100 mM Na^+ and 5 mM Ca^{2+} in the external solution, PCL was about five times more permeable to Ca^{2+} than to Na^+, at –50 mV in the activated state. In the resting state, with NaCl-containing solution, PCL was 4.3 ± 0.7 ($n = 10$) times more permeable to Ca^{2+} than to Na^+.

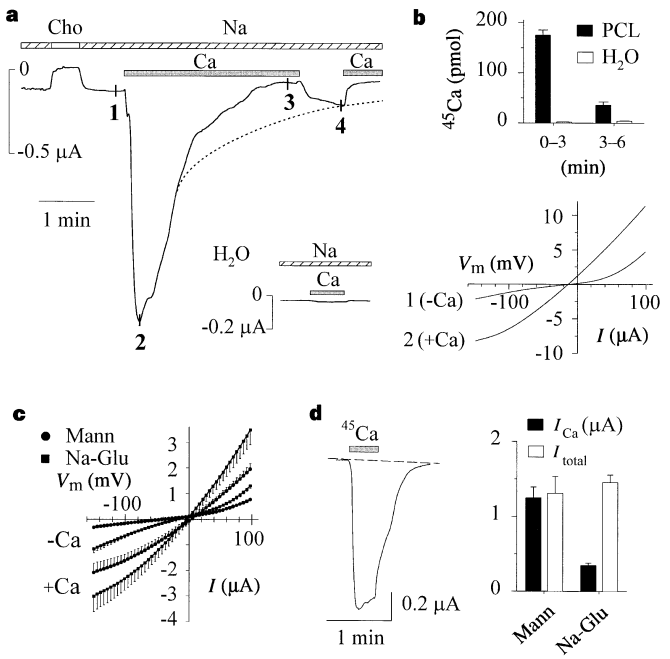

Figure 2 Polycystin-L conductance is stimulated by Ca^{2+}. **a**, Whole-cell currents recorded at –50 mV in the presence of choline-Cl-substituted (Cho) and NaCl-containing (Na) solutions. Addition of 5 mM $CaCl_2$ is indicated by grey bars. The dotted curve approximates the time course of the inward current when external Ca^{2+} was removed after the current reached its peak (point 2). The inset is a recording at –50 mV from an H_2O-injected oocyte. **b**, Top, ^{45}Ca uptake in oocytes pre-incubated in NaCl-containing solution for 10 min. Non-radioactive Ca^{2+} (5 mM) was added at time 0. 0–3 and 3–6 indicate the periods (in min) of ^{45}Ca incubation. Bottom, *I–V* curves obtained from the same oocyte before (point 1) or after (point 2) Ca^{2+} addition. **c**, Average *I–V* curves obtained before or after external Ca^{2+} addition, in Na-glutamate- (Na-Glu) or mannitol (Mann)-substituted solution, in the same oocytes ($n = 10$) pre-incubated in Cl^--free solution for >10 h. **d**, Left, current at –50 mV in mannitol-substituted solution before and after activation by 5 mM $^{45}CaCl_2$. Ca^{2+} uptake was then converted into current by taking the half-width of the spike as the uptake time. Right, calcium and total currents converted similarly in mannitol- or Na-glutamate-substituted solution ($n = 4$).

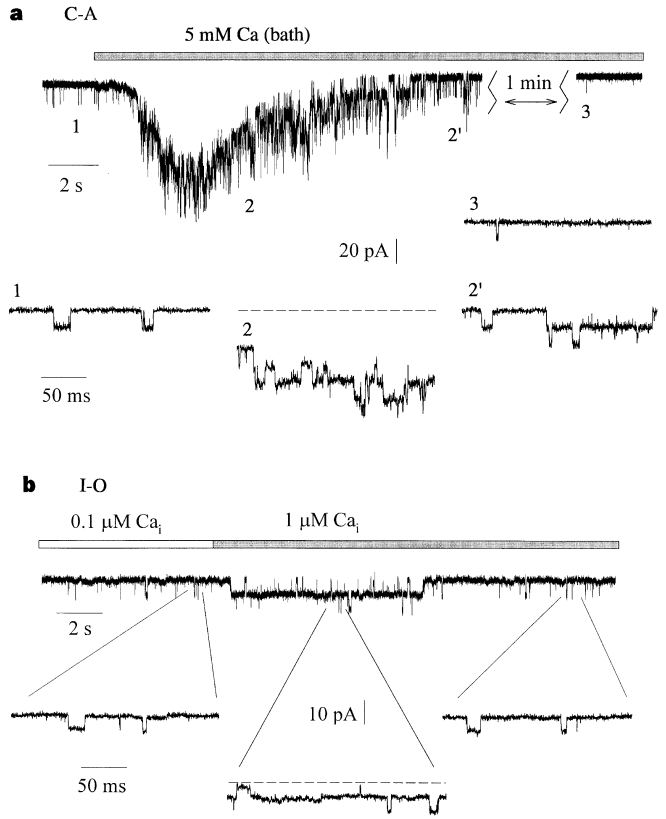

Figure 3 Activity of PCL single channels is increased by Ca^{2+}. **a**, Top, single-channel currents recorded at –60 mV in a cell-attached patch before and after adding 5 mM Ca^{2+} to the bath (Na_o solution). The pipette solution was $K140_o$. Bottom, expanded traces representing, respectively, the resting (1), activated (2, 2′) and desensitized (3) states. Resting potential of oocytes was assumed to be –30 mV. **b**, Representative traces at –50 mV in an inside-out patch before and after adding 1 μM Ca_i^{2+} (top). Selected traces are expanded (bottom). Open probabilities were 0.14 ± 0.03, 0.58 ± 0.12, and 0.10 ± 0.02 ($n = 8$), for the resting, activated and desensitized states, respectively. The pipette solution was Na_o and the intracellular solution was K_o supplemented with 5 $CaK_2EGTA + H_2K_2EGTA$ to obtain 0.1 or 1 μM free Ca^{2+}.

Patch-clamp experiments showed that elevating bath Ca^{2+} to 5 mM evoked pronounced, but transient, increases in PCL channel activity in cell-attached patches, although the single-channel conductance remained nearly unchanged (Fig. 3a). This effect of bath Ca^{2+} indicates that an increase in intracellular Ca^{2+} (Ca_i^{2+}) concentration may have triggered the activation. Moreover, during desensitization of the channel, the presence of bath Ca^{2+} resulted in lower single-channel activity than in the resting state (Fig. 3a, points 3 versus 1), consistent with whole-cell observations (Fig. 2a, points 3 versus 1). Direct activation of PCL channel activity by Ca_i^{2+} was shown in inside-out patches (Fig. 3b). Sustained high Ca_i^{2+} (1–10 μM) did not appear to prevent subsequent decreases in channel activity, although the time needed to reach this state varied.

To determine whether an increase in extracellular Ca^{2+} alone could also activate PCL channel activity, oocytes were injected with 50 nl of 50 mM EGTA, a Ca^{2+} chelator, at least 2 h before experiments. Currents due to addition of 5 mM Ca_o^{2+} were much lower than without EGTA and could be repeatedly generated (compare Figs 4a and 2a), indicating that elevating Ca_o^{2+} alone did not trigger activation or desensitization of the PCL channel. It remains to be established whether Ca^{2+}-induced activation and the ensuing desensitization of the channel result from effects of Ca_i^{2+} on the putative EF-hand within the carboxy terminus (Fig. 1a) or calmodulin[10], or from other mechanisms[13,14].

PCL is permeable to Ba^{2+} and Sr^{2+}, but barely permeable to Mg^{2+} (Fig. 4a). Ba^{2+}, Sr^{2+} and Ca^{2+} (80 mM) generated comparable whole-cell inward currents to that generated by 100 mM Na^+ in EGTA-injected oocytes (data not shown). The PCL single-channel inward conductance was 120–135 pS with 80 mM Ba^{2+}, Sr^{2+} or Ca^{2+}. However, its permeation to mono- and divalent cations is not additive, as divalent cations inhibited currents generated by Na^+. Whereas Ca_o^{2+} inhibited Na^+ currents over a wide voltage range (Fig. 4b), Mg^{2+} inhibited Na^+ currents, by reducing the PCL channel open probability, only at negative potentials (data not shown). Reciprocally, Na^+ inhibited Ca^{2+} influx (Figs 2d and 4b, right panels). Thus, competitive binding may occur between mono- and divalent cations, but not between permeant monovalent cations, as mixing Na^+ and K^+ in different ratios did not reduce PCL conductance. La^{3+}, Gd^{3+} (0.1 mM but not 20 μM) and flufenamate (0.5 mM but not 50 μM), which are inhibitors of nonselective cation channels[15,16], exhibited significant inhibitory effects (not shown). Protons also affect PCL channel activity, as low external pH decreased both its resting conductance and Ca^{2+}-activated currents (Fig. 4c).

Ca^{2+} entry was not significantly enhanced by treating oocytes expressing PCL with 1 μM thapsigargin for 2 h (ref. 17), indicating that PCL, unlike members of the TRP family, is not a store-operated capacitative calcium-entry channel. PCL channel activity appears not to be regulated by phosphorylation dependent on protein kinase A (PKA) or protein kinase C (PKC) as neither cyclic AMP nor phorbol myristate acetate significantly affected Ca^{2+} entry (data not shown).

This study shows that PCL is a Ca^{2+}-modulated, Ca^{2+}-permeable, nonselective cation channel. Its ion selectivity, large single-channel conductance and relatively long open time distinguish it from structurally related channels of the TRP family, voltage-gated Ca^{2+} and Na^+ channels[8–10,18,19] and known endogenous cation channels in *Xenopus* oocytes, including the stretch-activated cation channel and hyperpolarization-activated cation channel[20–22]. It is unlikely that the unique channel activity observed in PCL-expressing oocytes results from upregulation or modulation of an endogenous channel, as actinomycin D had no effects on the activity (data not shown).

PCL and polycystin-2 share structural features and it is likely that both possess channel properties. We hypothesize that alteration of these channels leads to the abnormal fluid secretion[23] and cellular proliferation that are hallmarks of polycystic kidney disease (PKD). PCL is not yet known to be mutated in PKD but its murine orthologue is removed by a large deletion in *Krd* mice that exhibit renal cysts and other defects[6]. Polycystins-1 and -2 bind each other[24,25], and it is possible that PCL also oligomerizes with another polycystin *in vivo*. Elucidating the channel properties of polycystins should provide new therapeutic strategies for PKD. □

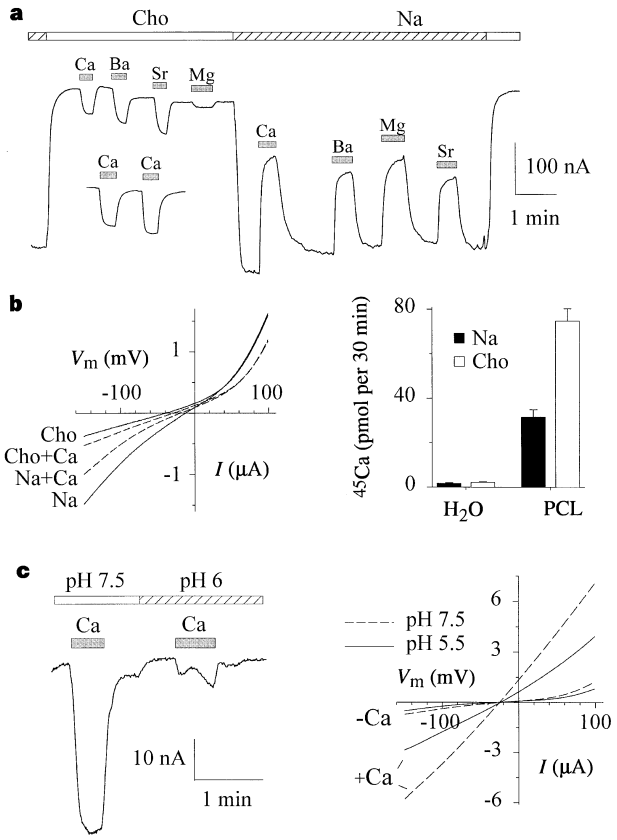

Figure 4 Effects of EGTA, divalent cations and protons. **a**, Currents recorded at –50 mV with an EGTA-injected oocyte in choline-Cl-substituted or NaCl-containing solution. External application of various divalent cations (5 mM) is indicated by grey bars. Inset, currents recorded with another oocyte in choline-Cl-substituted solution. **b**, Left, *I–V* relations obtained using EGTA-injected oocytes expressing PCL, before or after Ca^{2+} addition to choline-Cl-substituted or NaCl-containing solution. Right, $^{45}Ca^{2+}$ (1 mM) uptake using H_2O-injected or PCL-expressing oocytes, in NaCl-containing or choline-Cl-substituted solution. **c**, Left, currents recorded at –50 mV with EGTA-injected oocytes in NaCl-containing solution at indicated pH. Right, *I–V* curves obtained before or after adding 5 mM Ca^{2+} in NaCl-containing solutions in the same oocyte without EGTA injection.

Methods

Oocytic expression.

Capped synthetic RNA of human PCL[6] was synthesized by *in vitro* transcription from full-length cDNA in pTLN2 and injected (25–50 ng per oocyte) into *Xenopus laevis* oocytes prepared as described[26]. Equal volumes of H_2O were injected into control oocytes. Experiments were performed 1.5–4 days after injection.

Solutions.

Standard Barth's (or NaCl-containing) solution contained (in mM): 100 NaCl, 2 KCl, 1 $MgCl_2$, 10 Hepes, pH 7.5. When 100 mM NaCl was replaced with equimolar amounts of other salts, the resulting solutions were named accordingly; for example, Na-glutamate-substituted solution. 'Na_o', 'K_o' and '$K140_o$' indicate, respectively, extracellular (or pipette, in cell-attached and inside-out modes) solutions (100 NaCl, 2 KCl, 10 Hepes, pH 7.5; 100 KCl, 10 Hepes, pH 7.5; and 105 K-glutamate, 30 K-fluoride, 5 KCl, 5 EGTA, 5 Hepes, pH 7.3). 'Na_i', 'K_i' and '$NMDG_i$' indicate, respectively, intracellular (or pipette, in outside-out mode) solutions (100 NaCl, 2 KCl, 10 Hepes, pH 7.5; 100 KCl, 10 Hepes, pH 7.5; and 100 NMDG-Cl, 10 Hepes, pH 7.5). Cl^--free solution for oocyte pre-incubation contained: 80 Na-Hepes, 2 K-gluconate, 1 Mg-gluconate, 0.75 Ca-gluconate, and pH 7.5.

Electrophysiology.

Two-microelectrode voltage-clamp experiments were performed as described[27]. In experiments involving voltage ramping or holding, currents and voltages were digitized at 0.3 or 200 ms per sample and Bessel filtered at 10 or 0.02 kHz, respectively. We calculated ratios of permeability coefficients for monovalent cations using the equation derived from the GHK equation[28]: $P_X/P_{Na} = \exp(\Delta V_r/58.5)$, where ΔV_r (mV) is the change in reversal potential. To estimate the permeabilities of divalent cations relative to that of Na^+ under physiological conditions, we compared cation-evoked currents at −50 mV. Experimental results are expressed as mean ± s.e.m. (n). Patch-clamp experiments were performed as described[29]. We used a pipette-tip resistance of 5–10 MΩ and seal resistance of >10 GΩ. Single-channel currents were measured with an integrating patch-clamp amplifier, digitized at 0.15 ms per sample and filtered at 3 kHz through an 8-pole Bessel filter. To prevent possible run-down, cAMP, GTP-γ-S and ATP (0.1 mM) were added to intracellular solutions in most cases.

^{45}Ca-uptake measurements.

$^{45}CaCl_2$ of 30 and 60 μM, respectively, was added to uptake solutions containing 1 and 5 mM non-radioactive Ca^{2+}. 8–10 oocytes were incubated in 0.5 ml of uptake solution and uptake was terminated by washing oocytes in ice-cold NaCl-containing solution (pH 7.5). For experiments involving voltage-clamped ^{45}Ca uptake, Ca^{2+}-evoked currents and uptake of ^{45}Ca were simultaneously measured[30] at −50 mV.

Received 21 May; accepted 9 July 1999.

1. Gabow, P. A., Autosomal dominant polycystic kidney disease. *N. Engl. J. Med.* **329,** 332–342 (1993).
2. The European Polycystic Kidney Disease Consortium. The polycystic kidney disease 1 gene encodes a 14 kb transcript and lies within a duplicated region on chromosome 16. *Cell* **77,** 881–894 (1994).
3. The International Polycystic Kidney Disease Consortium. Polycystic kidney disease: the complete structure of the PKD1 gene and its protein. *Cell* **81,** 289–298 (1995).
4. Hughes, J. *et al*. The polycystic kidney disease 1 (PKD1) gene encodes a novel protein with multiple cell recognition domains. *Nature Genet.* **10,** 151–160 (1995).
5. Mochizuki, T. *et al*. PKD2, a gene for polycystic kidney disease that encodes an integral membrane protein. *Science* **272,** 1339–1342 (1996).
6. Nomura, H. *et al*. Identification of PKDL, a novel polycystic kidney disease 2-like gene whose murine homologue is deleted in mice with kidney and retinal defects. *J. Biol. Chem.* **273,** 25967–24973 (1998).
7. Wu, G. *et al*. Identification of PDK2L, a human PKD2-related gene: tissue-specific expression and mapping to chromosome 10q25. *Genomics* **54,** 564–568 (1998).
8. Kiselyov, K. *et al*. Functional interaction between InspP3 receptors and store-operated Htrp3 channels. *Nature* **396,** 478–482 (1998).
9. Perez-Reyes, E. *et al*. Molecular characterization of a neuronal low-voltage-activated T-type calcium channel. *Nature* **391,** 896–900 (1998).
10. Xia, X. M. *et al*. Mechanism of calcium gating in small-conductance calcium-activated potassium channels. *Nature* **395,** 503–507 (1998).
11. Jorgensen, A. J., Bennekou, P., Eskesen, K. & Kristensen, B. I. Annexins from Ehrlich ascites cells inhibit the calcium-activated chloride current in *Xenopus laevis* oocytes. *Pflugers Arch.* **434,** 261–266 (1997).
12. Boton, R., Dascal, N., Gillo, B. & Lass, Y. Two calcium-activated chloride conductances in *Xenopus laevis* oocytes permeabilized with the ionophore A23187. *J. Physiol. (Lond.)* **408,** 511–534 (1989).
13. Zitt, C. *et al*. Expression of TRPC3 in Chinese hamster ovary cells results in calcium-activated cation currents not related to store depletion. *J. Cell Biol.* **138,** 1333–1341 (1997).
14. Zuhlke, R. D. & Reuter, H. Ca^{2+}-sensitive desensitization of L-type Ca^{2+} channels depends on multiple cytoplasmic amino acid sequences of the α_{1C} subunit. *Proc. Natl Acad. Sci. USA* **95,** 3287–3294 (1998).
15. Gogelein, H., Dahlem, D., Englert, H. C. & Lang, H. J. Flufenamic acid, mefenamic acid and niflumic acid inhibit single nonselective cation channels in the rat exocrine pancreas. *FEBS Lett.* **268,** 79–82 (1990).
16. Kunze, D. L., Sinkins, W. G., Vaca, L. & Schilling, W. P. Properties of single *Drosophila* Trp1 channels expressed in Sf9 insect cells. *Am. J. Physiol.* **272,** C27–C34 (1997).
17. Gillo, B. *et al*. Coexpression of *Drosophila* TRP and TRP-like proteins in *Xenopus* oocytes reconstitutes capacitative Ca^{2+} entry. *Proc. Natl Acad. Sci. USA* **93,** 14146–14151 (1996).
18. Caterina, M. J. *et al*. The capsaicin receptor: a heat-activated ion channel in the pain pathway. *Nature* **389,** 816–824 (1997).
19. Birnbaumer, L. *et al*. On the molecular basis and regulation of cellular capacitative calcium entry: roles for TRP proteins. *Proc. Natl Acad. Sci. USA* **93,** 15195–15202 (1996).
20. Yang, X. C. & Sachs, F. Block of stretch-activated ion channels in *Xenopus* oocytes by gadolinium and calcium ions. *Science* **243,** 1068–1071 (1989).
21. Lane, J. W., McBride, D. W. Jr & Hamill, O. P. Ionic effects on amiloride block of the mechanosensitive channel in *Xenopus* oocytes. *Br. J. Pharmacol.* **108,** 116–119 (1993).
22. Tzounopoulos, T., Maylie, J. & Adelman, J. P. Induction of endogenous channels by high levels of heterologous membrane proteins in *Xenopus* oocytes. *Biophys. J.* **69,** 904–908 (1995).
23. Sullivan, L. P., Wallace, D. P. & Grantham, J. J. Chloride and fluid secretion in polycystic kidney disease. *J. Am. Soc. Nephrol.* **9,** 903–916 (1998).
24. Tsiokas, L., Kim, E., Arnould, T., Sukhatme, V. P. & Walz, G. Homo- and heterodimeric interactions between the gene products of PKD1 and PKD2. *Proc. Natl Acad. Sci. USA* **94,** 6965–6970 (1997).
25. Qian, F. *et al*. PKD1 interacts with PKD2 through a probable coiled-coil domain. *Nature Genet.* **16,** 179–183 (1997).
26. Saadi, I. *et al*. Molecular genetics of cystinuiria: mutation analysis of SLC3A1 and evidence for another gene in type I (silent) phenotype. *Kidney Int.* **54,** 48–55 (1998).
27. Chen, X.-Z., Shayakul, C., Berger, U. V., Tian, W. & Hediger, M. A. Characterization of a rat Na^+-dicarboxylate cotransporter. *J. Biol. Chem.* **273,** 20972–20981 (1998).
28. Hille, B. in *Ionic Channels of Excitable Membranes* (ed. Hille, B.) 105–108 (Sinauer, Sunderland, Massachusetts, 1992).
29. Hamill, O. P., Marty, A., Neher, E., Sakmann, B. & Sigworth, F. J. Improved patch-clamp techniques for high-resolution current recording from cells and cell-free membrane patches. *Pflugers Arch.* **391,** 85–100 (1981).
30. Chen, X.-Z., Zhu, T., Smith, D. E. & Hediger, M. A. Stoichiometry and kinetics of the rat high-affinity H^+-coupled peptide transporter PepT2. *J. Biol. Chem.* **274,** 2773–2779 (1999).

Acknowledgements

We thank P. Fong for providing pTLN2. X.-Z.C. is a recipient of the International Human Frontier Science Program Long-Term Fellowship. This work is supported by NARSAD and the Stanley Foundation (P.M.V.), the St. Giles Foundation (E.M.B.) and NIH (S.T.R., E.M.B., M.A.H. and J.Z.).

Correspondence and requests for materials should be addressed to J.Z. (e-mail: zhou@rics.bwh.harvard. edu) or M.A.H. (e-mail: mhediger@rics.bwh.harvard.edu).

A polycystic kidney-disease gene homologue required for male mating behaviour in *C. elegans*

Maureen M. Barr & Paul W. Sternberg

Howard Hughes Medical Institute and Division of Biology, California Institute of Technology, Pasadena, California 91125, USA

The stereotyped mating behaviour of the *Caenorhabditis elegans* male is made up of several substeps: response, backing, turning, vulva location, spicule insertion and sperm transfer. The complexity of this behaviour is reflected in the sexually dimorphic anatomy and nervous system[1]. Behavioural functions have been assigned to most of the male-specific sensory neurons by means of cell ablations; for example, the hook sensory neurons HOA and HOB are specifically required for vulva location[2]. We have investigated how sensory perception of the hermaphrodite by the *C. elegans* male controls mating behaviours. Here we identify a gene, *lov-1* (for location of vulva), that is required for two male sensory behaviours: response and vulva location. *lov-1* encodes a putative membrane protein with a mucin-like, serine–threonine-rich amino terminus[3] followed by two blocks of homology to human polycystins, products of the autosomal dominant polycystic kidney-disease loci PKD1 and PKD2 (ref 4). LOV-1 is the closest *C. elegans* homologue of PKD1. *lov-1* is expressed in adult males in sensory neurons of the rays, hook and head, which mediate response, vulva location, and potentially chemotaxis to hermaphrodites, respectively[2,5]. PKD-2, the *C. elegans* homologue of PKD2, is localized to the same neurons as LOV-1, suggesting that they function in the same pathway.

We examined the mating behaviour of existing mutants that are defective in sensory behaviours including mechanosensation, osmotic avoidance and chemotaxis to soluble and volatile odorants. Only males with severe defects in all sensory neuron cilia (*daf-10*, *osm-5*, *osm-6* and *che-3*) were defective of vulva location (Table 1); all cilia in *C. elegans* are in the dendritic endings of sensory neurons[5,6]. Only ciliated neurons express *osm-6::gfp*, with male-specific expression in four CEM head neurons and neurons of the rays and copulatory spicules[7]. Expression of *osm-6::gfp* begins at the L4 stage in neuronal cell bodies and extends to dendrites as neuronal outgrowth proceeds. The RnA and RnB neurons of each ray (rays 1–9), both HOA and HOB hook neurons, the spicule neurons SPV and SPD, and the PCB postcloacal sensilla neurons accumulate green fluorescent protein (GFP). OSM-6 may be required for the structure and function of ciliated neurons in the tail of the adult male, just as it is for neurons involved in many sensory behaviours[8,9].

By screening for mutants defective in vulva location, we identified *lov-1(sy552)*, which results in specific response and vulva-location